Persistent spin currents in a triple-terminal quantum ring with three arms*

Du Jian(杜坚)[1,†], Wang Suxin(王素新)[1], Pan Jianghong(潘江洪)[2], and Duan Xiuzhi(段秀芝)[3]

[1]Department of Physics, Hebei Normal College for Nationalities, Chengde 067000, China
[2]College of Physics and Technology, Guangxi Normal University, Guilin 541004, China
[3]College of Light Industry, Hebei Polytechnic University, Tangshan 063000, China

Abstract: A new model of a triple-terminal quantum ring with three arms is proposed. We develop an equivalent method for reducing the triple-terminal quantum ring to the double-terminal quantum ring and calculate the persistent spin currents in this model. The results indicate that the persistent spin currents show behavior of nonperiodic and unequal amplitude oscillation with increasing semiconductor ring size when the total magnetic flux is zero. However, when the total magnetic flux is non-zero, the persistent spin currents make periodic equal amplitude oscillations with increasing AB magnetic flux intensity. At the same time, the two kinds of spin state persistent spin currents have the same frequency and amplitude but the inverse phase. In addition, the Rashba spin-orbit interaction affects the phase and the phase difference of the persistent spin currents. The average persistent spin currents relate to the arm length and the terminal position as well as the distribution of the magnetic flux in each arm. Furthermore, our results indicate that the AB magnetic flux has different influences on the two kinds of spin state electrons.

1. Introduction

Taking advantage of spin properties, scientists improve the existing quantum device performance adding new functions, and manufacture a new generation of multifunctional spintronic devices through revolutionizing electrons[1−3]. Berry[4] first discovered the geometric phase in adiabatic cycliaction's Hamilton system, which provides a new method to study quantum structures. The Berry phase can be interpreted as a holonomy associated with the parallel transport around a circuit in a parameter space. The persistent currents induced by the Berry phase in textured microscopic rings were studied by Loss *et al.*[5]. In recent years, the spin-orbit interaction (SOI) in low-dimensional semiconductor structures has attracted much attention due to its potential applications in spintronic devices[6]. The Rashba spin-orbit interaction (RSOI) is induced by structure inversion asymmetry[7]. The strength of the RSOI can be tuned by external gate voltages or asymmetric doping. It provides us with a possibility to generate the spin current (SC) electrically without ferromagnetic metal or a magnetic field. In addition, the transmission properties of microscopic AB and AC rings have been widely studied[8−14]. Since the discovery of the persistent current, there have been many studies on the single ring, coupled ring, and connected ring structures[15−17]. This research discloses that the persistent current runs not only in isolated rings but also in an AB quantum ring with multiple arms[18, 19].

In this paper, a new model of a triple-terminal quantum ring with three arms is proposed. We develop an equivalent method to reduce this kind of model to a double-terminal AB ring. The properties of the persistent spin currents are investigated by using the new method. Our results further confirm that the AB magnetic flux and the Rashba spin-orbit interaction have an important effect on the persistent currents.

2. Model and formula

The model studied in this paper is a one-dimensional (1D) triple-terminal quantum ring with three arms, as shown in Fig. 1. The electron enters from the left terminal and goes out from the upper and the right terminal. Here, $\varphi' = -\varphi$, S and M denote semiconductor and nonferromagnetic, respectively. Considering the Rashba SOI, the Hamiltonian can be described as

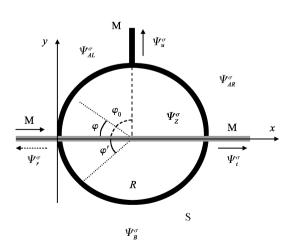$$\hat{H}_{so} = \frac{\alpha}{\hbar}(\hat{\boldsymbol{\sigma}} \times \hat{\boldsymbol{P}})_k, \tag{1}$$

Fig. 1. One-dimensional (1D) triple-terminal quantum ring with three arms. The relative position of the two leads is described by angle φ_0.

where $\hat{\boldsymbol{\sigma}} = (\sigma_x + \sigma_y + \sigma_z)$ are Pauli spin matrices and α is the RSOI parameter, whose range is $(0.5–2.0) \times 10^{-11}$ for an InGaAs-based semiconductor quantum ring. The total Hamiltonian with RSOI can be written as[20]

$$\hat{H} = \frac{2m_s^* R^2}{\hbar^2} \hat{H}_{1D} = \left(-i\frac{\partial}{\partial\varphi} + \frac{\beta}{2}\sigma_r - \frac{\Phi_{AB}}{\phi_0}\right)^2. \quad (2)$$

Here, m_s^* is the carrier effective mass, $\beta = 2\alpha m_s^*/\hbar^2$, $\sigma_r = \cos\varphi\sigma_i + \sin\varphi\sigma_j$, Φ_{AB} is AB magnetic flux, and $\phi_0 = hc/e$ is quantum flux. The energy eigenvalues in the AB ring can be obtained from Ref. [21] as

$$E_n^\sigma = \left(n - \Phi_{AC}^\sigma/2\pi - \Phi_{AB}/2\pi\right)^2. \quad (3)$$

Here, $\sigma = \pm 1$, $\Phi_{AC}^\sigma = -\pi\left(1 - \sigma\sqrt{\beta^2 + 1}\right)$ is the so-called Aharonov-Casher phase. For a given energy, the quantum numbers $n_\lambda^\sigma(E) = \lambda\sqrt{E} + \Phi^\sigma/2\pi = \lambda kR + \Phi^\sigma/2\pi$, and the index $\lambda = \pm$ refer to right and left movers, respectively. The eigenvectors have the general form $\Psi_n^\sigma(\varphi) = e^{in\varphi}\chi^\sigma(\varphi)$, and the mutually orthogonal spinors $\chi^\sigma(\varphi)$ can be expressed in terms of the eigenvectors of the Pauli matrix σ_k. We study the quantum ring structure applying the 1D quantum waveguide theory. When the distribution of the magnetic flux in the upper arm and the lower arm are in common, if an electron moves along the upper arm in the clockwise direction from the left terminal at $\varphi = 0$ to $\varphi = \pi/2$ (see Fig. 1), it acquires a phase $\Phi^\sigma/4$ at the output terminal, whereas the electron acquires a phase $-\Phi^\sigma/2$ in the counterclockwise direction along the lower arm when moving from $\varphi' = 0$ to $\varphi' = \pi$. In addition, it acquires zero phase at the right terminal when the electron moves along the middle arm. Assuming that the three nonferromagnetic leads are all ideal conductors and neglecting the scattering at the junctions, the functions in the upper and lower as well as the middle arms of the ring can be written as

$$\Psi_{AL,\sigma}^s(\varphi) = \sum_{\sigma=\pm,\lambda=\pm} c_{AL,\sigma}^\lambda e^{in_\lambda^\varphi \varphi}\chi^\sigma(\varphi), \quad (4)$$

$$\Psi_{AR,\sigma}^s(\varphi) = \sum_{\sigma=\pm,\lambda=\pm} c_{AR,\sigma}^\lambda e^{in_\lambda^\sigma \varphi}\chi^\sigma(\varphi), \quad (5)$$

$$\Psi_{Z,\sigma}^s(\varphi) = \sum_{\sigma=\pm,\lambda=\pm} c_{Z,\sigma}^\lambda e^{ik_\lambda^\sigma x}\chi^\sigma(\varphi), \quad (6)$$

$$\Psi_{B,\sigma}^s(\varphi') = \sum_{\sigma=\pm,\lambda=\pm} c_{B,\sigma}^\lambda e^{-in_\lambda^\sigma \varphi'}\chi^\sigma(\varphi'), \quad (7)$$

$$\Psi_\sigma^r = e^{ik_m x} + r_\sigma e^{-ik_m x}, \quad (8)$$

$$\Psi_\sigma^t = t_\sigma e^{ik_m x}, \quad (9)$$

$$\Psi_\sigma^u = u_\sigma e^{ik_m y}, \quad (10)$$

where $\chi^\uparrow(\varphi) = \frac{1}{\sqrt{2\pi}}\left(\begin{smallmatrix}\cos\vartheta/2\\ e^{i\varphi}\sin\vartheta/2\end{smallmatrix}\right)$ and $\chi^\downarrow(\varphi) = \frac{1}{\sqrt{2\pi}}\left(\begin{smallmatrix}\sin\vartheta/2\\ -e^{i\varphi}\cos\vartheta/2\end{smallmatrix}\right)$. In addition, r, t and u denote the left, the right and the upper metal lead, respectively, L and R denote the left and the right quantum ring, A and B denote the upper and the lower arm of the identical ring, respectively, r_σ is the spin-dependent reflection coefficient, u_σ and t_σ are the spin-dependent transmission coefficients, and k_m is the Fermi wave vector for the electrons in the three nonferromagnetic leads. Considering the spin rotation influence at the junction, the current density becomes

$$J^\sigma = \text{Re}\left[(\Psi^\sigma\chi^\sigma)^+ \left(-i\frac{\partial}{\partial\varphi} + \frac{\beta}{2\sigma_\gamma} - \frac{\Phi_{AB}}{\phi_0}\right)(\Psi^\sigma\chi^\sigma)\right]. \quad (11)$$

When the ring is connected to external leads, it is appropriate to apply the Griffith boundary condition at the intersection. Therefore, for $\varphi_0 = \pi/2$, the equations to be solved are

$$1 + r_\sigma = c_{AL\sigma}^+ + c_{AL\sigma}^- e^{-i\Phi^\sigma/4} = c_{Z\sigma}^+ + c_{Z\sigma}^- = c_{B\sigma}^+ + c_{B\sigma}^- e^{i\Phi^\sigma/2}, \quad (12)$$

$$u_\sigma e^{ik_m\phi/4k} = c_{AL\sigma}^+ e^{i(\phi+\Phi^\sigma)/4} + c_{AL\sigma}^- e^{-i\phi/4}$$
$$= c_{AR\sigma}^+ e^{i\phi/4} + c_{AR\sigma}^- e^{-i(\phi+\Phi^\sigma)/4}, \quad (13)$$

$$t_\sigma e^{ik_m\phi/\pi k} = c_{AR\sigma}^+ e^{i(2\phi+\Phi^\sigma)/4} + c_{AR\sigma}^- e^{-i\phi/2}$$
$$= c_{Z\sigma}^+ e^{i\phi/\pi} + c_{Z\sigma}^- e^{-i\phi/\pi}$$
$$= c_{B\sigma}^+ e^{i(\phi-\Phi^\sigma)/2} + c_{B\sigma}^- e^{-i\phi/2}, \quad (14)$$

$$k_m(1 - r_\sigma) = k(c_{AL\sigma}^+ - c_{AL\sigma}^- e^{-i\Phi^\sigma/4} + c_{Z\sigma}^+ - c_{Z\sigma}^- + c_{B\sigma}^+ - c_{B\sigma}^- e^{i\Phi^\sigma/2}), \quad (15)$$

$$k_m u_\sigma e^{ik_m\phi/4k} = k\left[c_{AL\sigma}^+ e^{i(\phi+\Phi^\sigma)/4} - c_{AL\sigma}^- e^{-i\phi/4} - c_{AR\sigma}^+ e^{i\phi/4} + c_{AR\sigma}^- e^{-i(\phi+\Phi^\sigma)/4}\right], \quad (16)$$

$$k_m t_\sigma e^{ik_m\phi/\pi k} = k\left[c_{AR\sigma}^+ e^{i(2\phi+\Phi^\sigma)/4} - c_{AR\sigma}^- e^{-i\phi/2} + c_{Z\sigma}^+ e^{i\phi/\pi} - c_{Z\sigma}^- e^{-i\phi/\pi} + c_{B\sigma}^+ e^{i(\phi-\Phi^\sigma)/2} - c_{B\sigma}^- e^{-i\phi/2}\right], \quad (17)$$

where $\phi = 2\pi kR = 2kL$. ϕ and kL are both physical quantities describing the quantum ring's size on account of $L = \pi R = \phi/2k$. Once t_σ and u_σ are obtained, the transmission probabilities for the right and the upper output terminals can be acquired from

$$T_t^\sigma = \frac{k_m^R}{k_m^L}|t_\sigma|^2, \quad (18)$$

$$T_u^\sigma = \frac{k_m^u}{k_m^L}|u_\sigma|^2. \quad (19)$$

We now study the current flow in the ring. The total current flow around a small energy interval is given by $I^\sigma = \frac{e}{2\pi\hbar}T^\sigma$. For the double-arm quantum ring, the total current is $I^\sigma = I_A^\sigma + I_B^\sigma$. It is noted that the current in the upper and lower arm is $I_A^\sigma = I^\sigma + I_P^\sigma$ and $I_B^\sigma = -I_P^\sigma$, respectively. The current in each arm is generally different from the others in the identical ring because of symmetry breaking via the AB effect and of the unequal arm length. Therefore, we can define the persistent spin currents in the double-arm ring as $I_P^\sigma = \left(I^\sigma - |I_A^\sigma| - |I_B^\sigma|\right)/2$. In order to investigate the persistent spin currents in each arm, we develop an equivalent method as follows. Firstly, we take the upper lead and the right lead as well as the right part of the upper arm as a whole, which can be viewed as an equivalent junction. Then taking the total currents in the ring as the sum of the currents in the upper lead and the right lead ($I^\sigma = I_t^\sigma + I_u^\sigma$), so the triple-terminal quantum ring with three arms reduces to a double-terminal quantum ring with three arms. Certainly, the new equivalent junction is only an assumption. In fact, it is a whole structure taking up
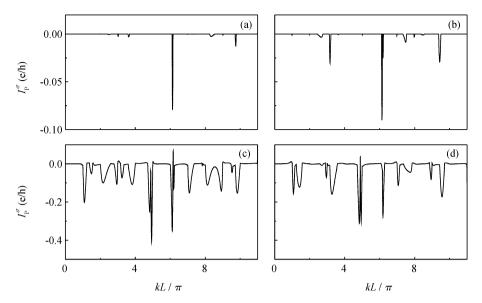
Fig. 2. Persistent spin currents as functions of kL/π in each arm with $\Phi^\sigma = 0$ for (a) I^σ_{ALP}, $\varphi_0 = \pi/2$; (b) I^σ_{ALP}, $\varphi_0 = 2\pi/3$; (c) I^σ_{ZP}, $\varphi_0 = \pi/2$; (d) I^σ_{BP}, $\varphi_0 = \pi/2$, where the solid and the dotted lines correspond to $\sigma = \uparrow, \downarrow$, respectively.

space and the left part of the upper arm does not become longer as well the right does not become shorter. Therefore, for the same magnetic flux distribution, the persistent spin current in each arm is not changed. If taking the middle and the lower arm as an equivalent single arm[18], and neglecting the circling current between the middle arm and the lower one, we can further simplify the calculation of the persistent spin currents in a triple-arm quantum ring as a double-arm quantum ring[18].

By applying the boundary conditions at the junctions and the conservation of the currents, we achieved a set of equations that can be solved, and the probability current density in each arm is obtained. Assuming such probability current I^σ is charged current corresponding to the probability current density J^σ, the probability current in the three arms can be written as

$$I^\sigma_{\text{AL}} = \frac{k}{k_{\text{m}}} \left(|c^+_{\text{AL}\sigma}|^2 - |c^-_{\text{AL}\sigma}|^2 \right), \qquad (20)$$

$$I^\sigma_{\text{AR}} = \frac{k}{k_{\text{m}}} \left(|c^+_{\text{AR}\sigma}|^2 - |c^-_{\text{AR}\sigma}|^2 \right), \qquad (21)$$

$$I^\sigma_{\text{Z}} = \frac{k}{k_{\text{m}}} \left(|c^+_{\text{Z}\sigma}|^2 - |c^-_{\text{Z}\sigma}|^2 \right), \qquad (22)$$

$$I^\sigma_{\text{B}} = \frac{k}{k_{\text{m}}} \left(|c^+_{\text{B}\sigma}|^2 - |c^-_{\text{B}\sigma}|^2 \right). \qquad (23)$$

Here, I^σ_{AL} is the probability current in the left part of the upper arm. According to the conservation of the currents at the junction, the effective probability current in the new equivalent single arm can be defined as

$$I^\sigma_{\text{effA}} = \frac{k}{k_{\text{m}}} \left(|c^+_{\text{Z}\sigma}|^2 - |c^-_{\text{Z}\sigma}|^2 + |c^+_{\text{B}\sigma}|^2 - |c^-_{\text{B}\sigma}|^2 \right). \qquad (24)$$

Assuming the total current flowing from the new junction is $I^\sigma = I^\sigma_{\text{t}} + I^\sigma_{\text{u}}$, the probability current flowing from the left part of the upper arm to the new junction is I^σ_{AL}. In addition, I^σ_{effA} is the probability current flowing from the new equivalent

single arm to the new junction. We define the persistent spin current in the left part of the upper arm as

$$I^\sigma_{\text{ALP}} = \left(I^\sigma_{\text{u}} + I^\sigma_{\text{t}} - |I^\sigma_{\text{AL}}| - |I^\sigma_{\text{effA}}| \right)/2. \qquad (25)$$

Using the same method, we can obtain the effective probability current I^σ_{effZ} and I^σ_{effB} as well as the persistent spin currents I^σ_{ZP} and I^σ_{BP} for the middle and the lower arms, as follows,

$$I^\sigma_{\text{effZ}} = \frac{k}{k_{\text{m}}} \left(|c^+_{\text{AL}\sigma}|^2 - |c^-_{\text{AL}\sigma}|^2 + |c^+_{\text{B}\sigma}|^2 - |c^-_{\text{B}\sigma}|^2 \right), \qquad (26)$$

$$I^\sigma_{\text{effB}} = \frac{k}{k_{\text{m}}} \left(|c^+_{\text{Z}\sigma}|^2 - |c^-_{\text{Z}\sigma}|^2 + |c^+_{\text{AL}\sigma}|^2 - |c^-_{\text{AL}\sigma}|^2 \right), \qquad (27)$$

$$I^\sigma_{\text{ZP}} = \left(I^\sigma_{\text{u}} + I^\sigma_{\text{t}} - |I^\sigma_{\text{Z}}| - |I^\sigma_{\text{effZ}}| \right)/2, \qquad (28)$$

$$I^\sigma_{\text{BP}} = \left(I^\sigma_{\text{u}} + I^\sigma_{\text{t}} - |I^\sigma_{\text{B}}| - |I^\sigma_{\text{effB}}| \right)/2. \qquad (29)$$

However, the persistent spin current in the right part of the upper arm cannot be calculated by using this kind of method, because these two kinds of models are different in terminals.

3. Results and analysis

As shown in Fig. 2, the numerical results of the persistent spin currents as functions of kL/π in each arm are presented with, $\Phi^\sigma = 0$, and φ_0 is set to be (a) $\varphi_0 = \pi/2$; (b) $\varphi_0 = 2\pi/3$; (c) $\varphi_0 = \pi/2$ and (d) $\varphi_0 = \pi/2$, respectively. The persistent spin currents show nonperiodic unequal amplitude oscillation with increasing semiconductor ring size. But the distributions of the resonance peaks (see Fig. 2 upside down) in every arm are almost same. This indicates that the persistent spin current is a resonance phenomenon occurring in the whole quantum ring, which only appears under specific sizes. Affected by the size effect, the middle and lower arms are different greatly in persistent spin current due to the different arm length. In Fig. 2, it is evident that the whole vibration curves for spin-up electrons coincide closely with spin-down
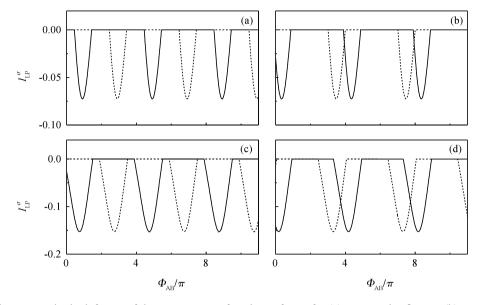
Fig. 3. Persistent spin currents in the left part of the upper arm as functions of ϕ_{AB} for (a) $\varphi_0 = \pi/2$, $\beta = 0$; (b) $\varphi_0 = \pi/2$, $\beta = 1.2$; (c) $\varphi_0 = 2\pi/3$, $\beta = 0$ and (d) $\varphi_0 = 2\pi/3$, $\beta = 1.2$, where the solid and the dotted lines correspond to $\sigma = \uparrow, \downarrow$, respectively.
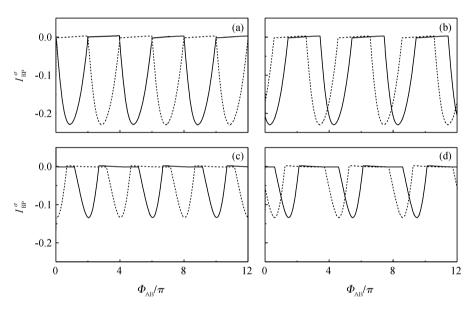

Fig. 4. Persistent spin currents in the lower arm as functions of ϕ_{AB} for (a) $kL = 5\pi$, $\beta = 0$; (b) $kL = 5\pi$, $\beta = 1.2$; (c) $kL = 4.5\pi$, $\beta = 0$ and (d) $kL = 4.5\pi$, $\beta = 1.2$, where the solid and the dotted lines correspond to $\sigma = \uparrow, \downarrow$, respectively.

ones when the angle φ_0 changes. This can be expressed as follows. There is no spin exchange splitting energy in the metal lead, so the two kinds of spin state electrons meet with the same obstruction in the transmission process. In addition, when angle φ_0 changes from $\varphi_0 = \pi/2$ to $\varphi_0 = 2\pi/3$, the number of peaks for the left part of the upper arm increases because the arm length becomes longer. Further, the average value of persistent spin currents becomes larger in this case. It is clear that the number of peaks for the left part of the upper arm is less than that for the lower or middle arm. The amplitude of the persistent spin current is lower too. This means that the average value of persistent spin current for the left part of the upper arm is less than that of the lower or middle one. The reason is that there exists an upper lead on the upper arm. This finding may be helpful for the application design.

In order to further understand the persistent spin currents

in the left part of the upper arm, we present the persistent spin currents in the left part of the upper arm as functions of ϕ_{AB} for (a) $\varphi_0 = \pi/2$, $\beta = 0$, (b) $\varphi_0 = \pi/2$, $\beta = 1.2$, (c) $\varphi_0 = 2\pi/3$, $\beta = 0$ and (d) $\varphi_0 = 2\pi/3$, $\beta = 1.2$, respectively. The numerical results are plotted in Fig. 3. It is seen that the persistent spin currents show periodic equal amplitude oscillations with increasing AB flux intensity. Further, the two kinds of spin state persistent currents have the identical amplitude and the inverse phase. As is known, there is no spin exchange splitting energy in the nonferromagnetic, so each terminal makes a similar contribution to the two kinds of spin state electrons, which lead to the identical amplitude. However, the AB flux has a different effect on the two kinds of spin state electrons due to the spin orientation being parallel or antiparallel to the external magnetic field. Comparing the small chart in Fig. 3(a) against Fig. 3(b), we can see that the shapes and the height of
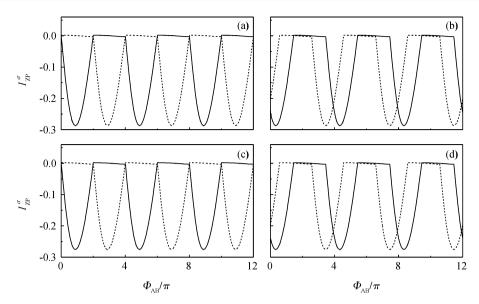
Fig. 5. Persistent spin current in the middle arm functions of ϕ_{AB} for (a) $\varphi_0 = \pi/2$, $\beta = 0$; (b) $\varphi_0 = \pi/2$, $\beta = 1.2$; (c) $\varphi_0 = 2\pi/3$, $\beta = 0$; (d) $\varphi_0 = 2\pi/3$, $\beta = 1.2$, where the solid and the dotted lines correspond to $\sigma = \uparrow, \downarrow$, respectively.

the resonant peaks (see Fig. 3 upside down) for the two kinds of persistent spin currents are the same, but the position of the peaks shifts. These results indicate that the Rashba spin-orbit interaction has an effect on changing the phase and the phase difference of the two kinds of persistent spin currents. Moreover, comparing the small chart in Figs. 3(a) and 3(b) against Figs. 3(c) and 3(d), when φ_0 changes from $\varphi_0 = \pi/2$ to $\varphi_0 = 2\pi/3$, one can see the shape of the resonant peaks becomes higher and fatter but the position shifts a little. This indicates that when the upper terminal closes from left clockwise to the right terminal, the two kinds of average persistent currents increase dramatically but the phase changes a little, and the phase difference retains the former value.

Figure 4 shows the persistent spin currents in the lower arm. Comparing the small chart in Figs. 4(a) and 4(b) with Figs. 3(a) and 3(b), we can see that the average persistent spin current in the lower arm is larger than that in upper one for the lack of a terminal in it. Comparing the small chart in Figs. 4(a) and 4(b) with Figs. 4(c) and 4(d), it can be found that the size of the quantum ring has an effect on the amplitude and phase of the two kinds of persistent spin currents, but it does not affect the phase difference. From chart (a) and (c) in Figs. 3 and 4, we can also find that when the Rashba spin-orbit interaction is absent, the two kinds of the persistent spin currents are separate. This may be helpful for the ringed spintronic device application design.

Figure 5 shows the persistent spin currents in the middle arm as functions of ϕ_{AB} in the present of Rashba spin-orbit interaction. It is obvious that the average persistent spin current in the middle arm is larger than that in the lower arm, which is caused by the different arm length and magnetic flux distribution in each arm. Further, changing angle has just a little effect on the persistent spin current in the middle arm.

4. Conclusions

In summary, a new model of a triple-terminal quantum ring with three arms has been proposed in this paper. By using a new equivalent junction method, persistent spin current properties are investigated. The results indicate that the persistent spin currents show the behavior of nonperiodic and unequal amplitude oscillation with increasing semiconductor ring size when the total magnetic flux is zero. However, when the total magnetic flux is non-zero, the persistent spin currents make periodic equal amplitude oscillations with increasing AB magnetic flux intension. The two kinds of persistent spin currents have the same frequency and the same amplitude but the inverse phase. The Rashba spin-orbit interaction concerns the phase and the phase difference of the persistent spin currents. The average persistent spin currents are related to the arm length and the arm position as well as the distribution of the magnetic flux in each arm. Furthermore, our results indicate that the persistent currents for the two kinds of spin state electrons are separate and the AB magnetic flux has different influences on them.

References

[1] Baibich M N, Broto J M, Fert J M, et al. Giant magnetoresistance of (001)Fe/(001)Cr magnetic superlattices. Phys Rev Lett, 1998, 61: 2472

[2] Slonczewski J C. Conductance and exchange coupling of two ferromagnets separated by a tunneling barrier. Phys Rev B, 1989, 39: 6995

[3] Viret M, Berger S, Gabureac M, et al. Magnetoresistance through a single nickel atom. Phys Rev B, 2002, 66: 220401

[4] Berry M V. Quantal phase factors accompanying adiabatic changes. Proc R Soc Lond A, 1984, 392: 45

[5] Loss D, Goldbart P, Balatsky A V. Berry's phase and persistent charge and spin currents in textured mesoscopic rings. Phys Rev Lett, 1990, 65: 1655

[6] Tsitsishvili E, Lozano G S, Gogolin A O. Rashba coupling in quantum dots: an exact solution. Phys Rev B, 2004, 70: 115316

[7] Bychkov Y A, Rashba E I. The internal pressures of liquids. J Phys, 1984, C17: 6039

[8] Büttiker M, Imry I, Azbel M Y. Quantum oscillations in one-

dimensional normal-metal rings. Phys Rev A, 1982, 30: 1982

[9] Aronov A G, Lyanda-Geller Y B. Spin-orbit Berry phase in conducting rings. Phys Rev Lett, 1993, 70: 343

[10] Qian T Z, Su Z B. Spin-orbit interaction and Aharonov-Anandan phase in mesoscopic rings. Phys Rev Lett, 1994, 72: 2311

[11] Nitta J, Meijer F E, Takayanagi H. Spin-interference device. Appl Phys Lett, 1999, 75: 695

[12] Frustaglia D, Richter K. Spin interference effects in ring conductors subject to Rashba coupling. Phys Rev B, 2004, 69: 235310

[13] Aeberhard U, Wakabayashi K, Sigrist M. Effect of spin-orbit coupling on the zero-conductance resonances in asymmetrically coupled one-dimensional rings. Phys Rev B, 2005, 72: 075382

[14] Foldi P, Molnar B, Benedict M G, et al. Spintronic single-qubit gate based on a quantum ring with spin-orbit interaction. Phys Rev B, 2005, 71: 033309

[15] Splettstoesser J, Governale M, Zulicke U. Persistent current in ballistic mesoscopic rings with Rashba spin-orbit coupling. Phys Rev B, 2003, 68: 165341

[16] Zhang Y T, Guo Y, Li Y C. Persistent spin currents in a quantum ring with multiple arms in the presence of spin-orbit interaction. Phys Rev B, 2005, 72: 125334

[17] Pletyukhov M, Gritsev V. Application, persistent currents in a multicomponent Tomonaga-Luttinger liquid: to a mesoscopic semiconductor ring with spin-orbit interaction. Phys Rev B, 2004, 70: 165316

[18] Wu H C, Guo Y, Chen X Y, et al. Giant persistent current in a quantum ring with multiple arms. Phys Rev B, 2003, 68: 125330

[19] Citro R, Romeo F, Marinaro M. Zero-conductance resonances and spin filtering effects in ringconductors subject to Rashba coupling. Phys Rev B, 2006, 74: 115329

[20] Meijer F E, Morpurgo A F, Klapwijk T M. One-dimensional ring in the presence of Rashba spin-orbit interaction: derivation of the correct Hamiltonian. Phys Rev B, 2002, 66: 033107

[21] Molnar B, Peeters F M, Vasilopoulos P. Spin-dependent magnetotransport through a ring due to spin-orbit interaction. Phys Rev B, 2004, 69: 155335